Ground-penetrating radar measurements of 64 Austrian glaciers between 1995 and 2010

Andrea FISCHER,[1] Michael KUHN[2]

[1]*Institute for Interdisciplinary Mountain Research, Austrian Academy of Sciences, Innsbruck, Austria*
E-mail: andrea.fischer@uibk.ac.at
[2]*University of Innsbruck, Innsbruck, Austria*

ABSTRACT. The ongoing retreat of mountain glaciers necessitates the development of future scenarios of glacier runoff. These scenarios are not only governed by future climate scenarios influencing glacier mass balance but also by the glacier volumes, which are subject to melt. Ground-penetrating radar (GPR) is a valuable tool for measuring the thickness of mountain glaciers, although ground-based measurements are labour-intensive, so not all glaciers can be surveyed. This study presents the results of GPR surveys on 64 Alpine glaciers, carried out between 1995 and 2010. The glacier areas range from 0.001 to 18.4 km^2, and their ice thickness was surveyed with an average density of 36 points km^{-2}. The point measurements were extrapolated manually to derive volume maps. The mean ice thickness varies between 10 and 92 m; the maximum ice thickness is about three times the mean thickness. According to the glacier state recorded in the second glacier inventory, the 64 glaciers cover an area of 223.3 ± 3.6 km^2, with a mean thickness of 50 ± 3 m and a glacier volume of 11.9 ± 1.1 km^3. The mean maximum ice thickness is 119 ± 5 m.

INTRODUCTION

The recent retreat of the world's glaciers (e.g. Lemke and others, 2007) affects hydrology on a local, regional and global scale (e.g. Arendt and others, 2002; Jansson and others, 2003; Kuhn and Escher-Vetter, 2004; Raper and Braithwaite, 2006; Casassa and others, 2009; Kaser and others, 2010; Radić and Hock, 2011). On a global scale, the runoff from mountain glaciers contributes to global sea-level rise. Regionally, the total amount and seasonality of the glacier runoff may change, with implications for water management, irrigation and energy production. Locally (e.g. in the European Alps), the glaciers as characteristic features of the landscape play a role in summer and winter tourism (Fischer and others, 2011). The possible disappearance of Alpine glaciers and the timescale for this (Zemp and others, 2006; Huss and others, 2008) are discussed with respect to all the issues mentioned above.

To monitor the past and current glacier changes, glacier areas, volume changes and mass balances are recorded using different methods. Glacier volume is an important initial condition for assessing further glacier retreat (Farinotti and others, 2009a). Furthermore, the total glacier volume is equal to the maximum potential contribution to sea-level rise. The pace of glacier retreat is not only governed by atmospheric conditions that influence mass balance, but also by the distribution of ice within the glacier, which controls the area loss and thus the area contributing to further ice melt.

Several glacier inventories include glacier volumes (e.g. Müller and others, 1976, 1977; WGMS, 1989), which are partly estimated or modelled. For the 1998 Austrian glacier inventory (Lambrecht and Kuhn, 2007; Kuhn and others, 2009, 2012), GPR measurements were carried out for two reasons: (1) to include measured volume data and (2) to improve the calculation of glacier volumes of unmeasured glaciers by surveying glaciers that are representative for all Austrian glaciers in terms of area, type, aspect and specific regions and slope. Ice thickness measurements started in 1995. Since ground-based measurements turned out to be labour-intensive and restricted by field conditions, the most recent surveys were carried out in 2010, 8 years after the previous data acquisitions for the glacier inventory. Of the 896 Austrian glaciers, 64 were measured (Kuhn and Fischer, 2012). To calculate the bedrock elevation from measured ice thickness data, digital elevation models (DEMs) of the glacier surface were used, which date from 1996–2002. Compilation of a third Austrian glacier inventory (GI III) is under way (Abermann and others, 2009, 2012; Stocker-Waldhuber and others, 2012), so that surface elevation changes before and after the second glacier inventory (GI II) and the radar survey can be estimated.

So far, several studies have been published describing specific aspects of the GPR measurements within GI II: the method for deriving point ice thickness and most of the measured point data is summarized by Span and others (2005) and Fischer and others, (2007). In a case study of one of the best-surveyed glaciers, Schaufelferner in the Stubai Alps, Fischer (2009) described different interpolation methods to calculate ice thickness for the total glacier area. Kuhn and Fischer (2012) summarized preliminary results for glacier volumes in the context of the 1998 glacier inventory.

In this paper, technical aspects, methods and assumptions are presented, with a rough assessment of the accuracy of the resulting ice volumes.

METHOD

Point ice thickness measurements

Ice thickness measurements were carried out with the transmitter developed by Narod and Clarke (1994) combined with resistively loaded dipole antennas (Wu and King, 1965; Rose and Vickers, 1974) at central wavelengths of 6.5 (30 m antenna length) and 4.0 MHz (50 m antenna length). The signal was recorded trace by trace with an oscilloscope. Examples of signals are provided in Figure 1, showing traces recorded at Schaufelferner in August 2006.

https://doi.org/10.3189/2013AoG64A108 Published online by Cambridge University Press

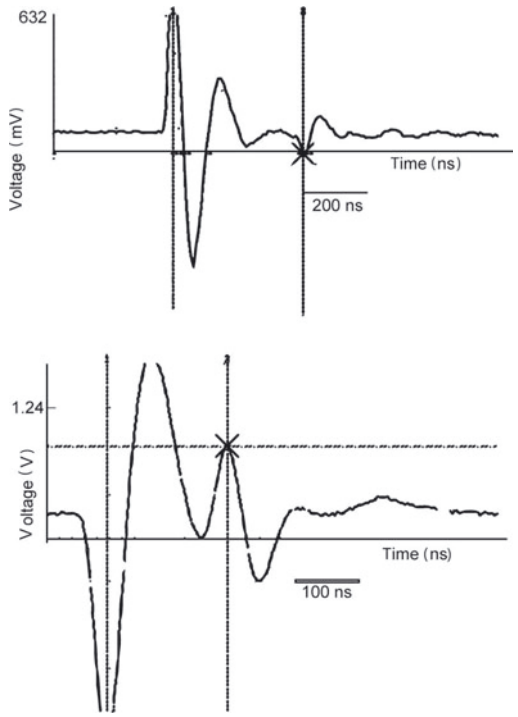

Fig. 1. Examples of GPR point records recorded with the Fluke 105 B oscilloscope on Schauferner in 2006.

The point ice thickness, h_p, was calculated for each measurement assuming a homogeneous plane-parallel ice block:

$$h_p = \frac{1}{2}\sqrt{\left(\Delta t + \frac{1}{c_a}\right)^2 c_i^2 - a^2}, \quad (1)$$

where Δt is the time difference between the direct and reflected signal and a is the antenna separation. The signal velocity in the glacier, c_i, is assumed to be 168 m µs^{-1} as used by Haeberli and others (1982), Narod and Clarke (1994) and Bauder (2001), and the signal velocity in air, c_a, is assumed to be 300 m µs^{-1}.

At the time of the measurements, the glaciers were covered with winter snow. In the accumulation area, firn cover existed until 2003 but then decreased sharply, with extremely high melt rates even at high elevations. Since the amounts of snow and firn cover vary for the specific measurement locations, and neither layer-thickness nor common-midpoint measurements been carried out frequently, the glacier was assumed to consist of ice when calculating the ice thickness with Eqn (1).

The measurement positions were recorded with a hand-held GPS with a nominal accuracy of 5–30 m depending on the number and position of satellites. Typically, the point measurements were located along several profiles across the glacier and, at the location of the maximum depth, along the glacier, with the aim of finding the maximum ice thickness. Examples of measured data are shown for Taschachferner and Mittelbergferner, Ötztal Alps, in Figure 2.

Data interpolation

The point measurements were interpolated to calculate the total glacier volume. As shown in Figure 2, the measured point data are often sparse and unequally distributed over the glacier. Additional information is drawn from the natural boundary condition that the ice thickness is zero at the glacier margins. However, in regions with sparse data, automatic interpolation with algorithms (e.g. kriging, inverse distance weighting (IDW) or spline) produces ice thickness maps that deviate considerably from what can be expected from an educated guess. For example, crevassed areas can indicate discontinuities in the bedrock, and ice thickness in steep areas is usually smaller than in neighbouring flat areas. Furthermore, slopes of side-walls exposed during recent

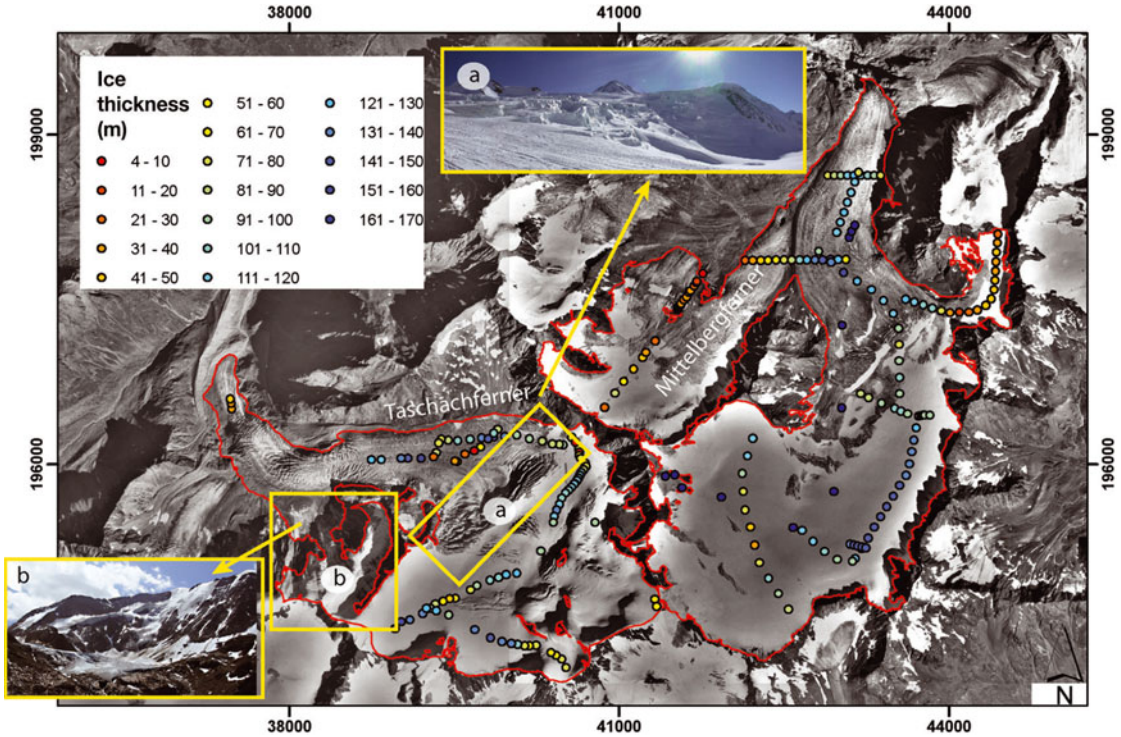

Fig. 2. Spatial distribution and results of ice thickness measurements for Mittelbergferner and Taschachferner in the Ötztal Alps. Data gaps on Taschachferner result from large crevasse zones and steep areas (small photographs).

https://doi.org/10.3189/2013AoG64A108 Published online by Cambridge University Press

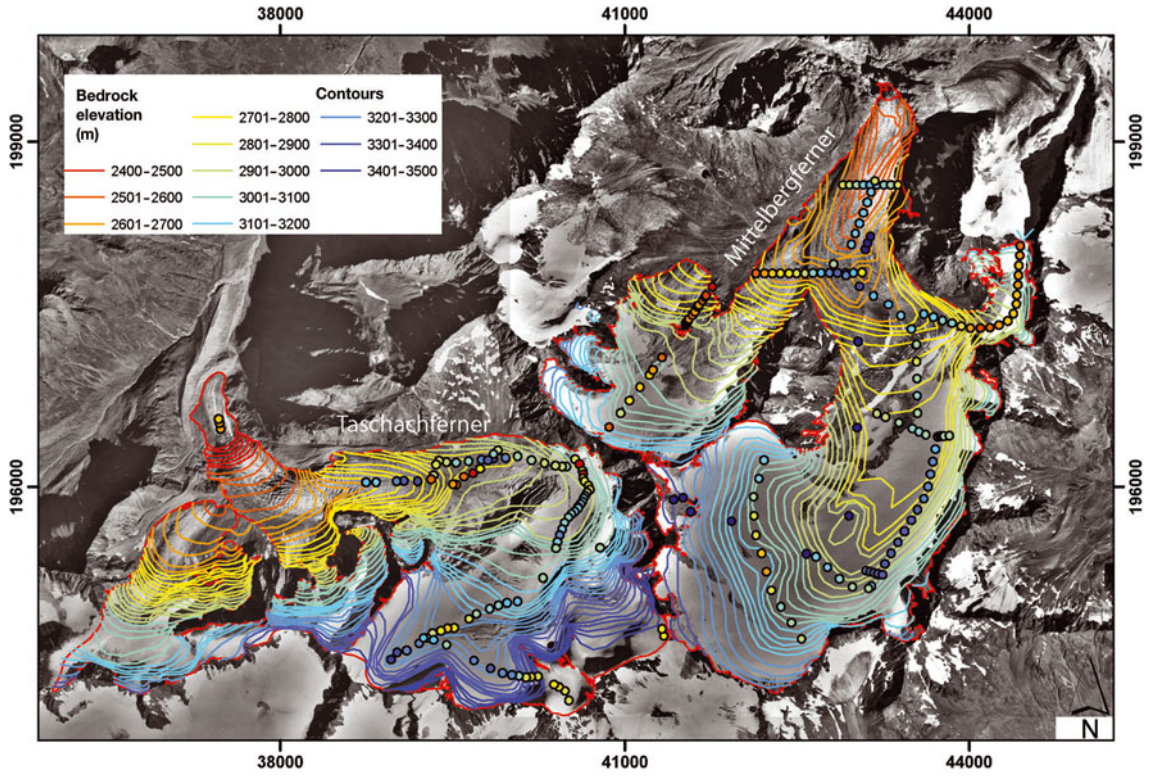

Fig. 3. 20 m contours of subglacial topography manually interpolated from the ice thickness measurements of Taschachferner and Mittelbergferner.

glacier retreat often suggest a constant slope, so the slope of the rocks surrounding the glaciers also provides information on the still ice-covered slope of the glacier bed. For hanging glaciers, the ice thickness at the front is apparent from the DEM of the glacier surface and the bedrock beneath. This information can be included, either by introducing artificial points for use in spatial interpolation algorithms or during manual construction of contours.

Another possibility is to interpolate measured data with the help of ice-dynamical models (e.g. Binder and others, 2009; Farinotti, 2009b). As the point data available for this study show inhomogeneous spatial distribution, and the method applied should be the same for every glacier, no such models have been used. Instead, 20 m contours of bedrock elevation were manually drawn (Fig. 3) for Taschachferner and Mittelbergferner according to point measurements and the following additional rules:

1. the ice thickness at glacier margins is zero
2. crevassed zones indicate ice thickness smaller than surrounding areas without crevasses
3. the slope of the surrounding bedrock indicates the slope of neighbouring ice-covered bedrock

These contours were then interpolated with the ArcGIS tool 'topo2raster' on a $5 \times 5\,m^2$ grid (Fig. 4). The topo2raster tool is based on the ANUDEM algorithm developed by Hutchinson (1989). The ice thickness was then derived by subtracting the bedrock elevation DEM from the surface elevation DEM (using the ArcGIS tool 'Minus'). The *z*-values of the nodes of the shapes of the glacier areas (without ice divides) were set to the value of surface elevation DEMs. Due to the difference between raster cells and node positions, the topo2raster interpolation often results in slightly negative ice thickness values. This was corrected by reclassification of these cells to an ice thickness of 2 m. The mean ice thickness, h, was calculated as the mean of the ice thickness, h_N, at all N gridcells, and the maximum ice thickness as the maximum of all gridcells. The volume, V, of a specific glacier was calculated by multiplying the mean ice thickness, h, by the glacier area, A.

Since all the volume data are intended for use in the glacier inventory, the area was taken from the glacier inventory even though the area changed between the GPR measurement and the date of the inventory. Thus the area assumed at the time of the measurements is too large, resulting in overestimation of the ice volume.

Uncertainty analysis

A rigorous and complete assesment of all errors and the uncertainty of the presented data based on sparse measurements would require a more thorough knowledge of a 'true value'. What can be done to allow at least an estimate of the reliability of the presented volumes is an uncertainty analysis of (1) case studies and (2) the specific components leading to the results at point and glacier-wide level.

Calculation of the volume involves deriving the mean ice thickness for the glacier area by extrapolating the point measurements, and multiplying it by the glacier area. Thus the uncertainty involved in these two steps must be investigated.

Uncertainty of point ice thickness measurements

The ice thickness at one measurement location is calculated using Eqn (1) and involves mainly the following uncertainties:

1. the uncertainty of the signal velocity in the glacier, mainly due to the neglected firn and snow layers

https://doi.org/10.3189/2013AoG64A108 Published online by Cambridge University Press

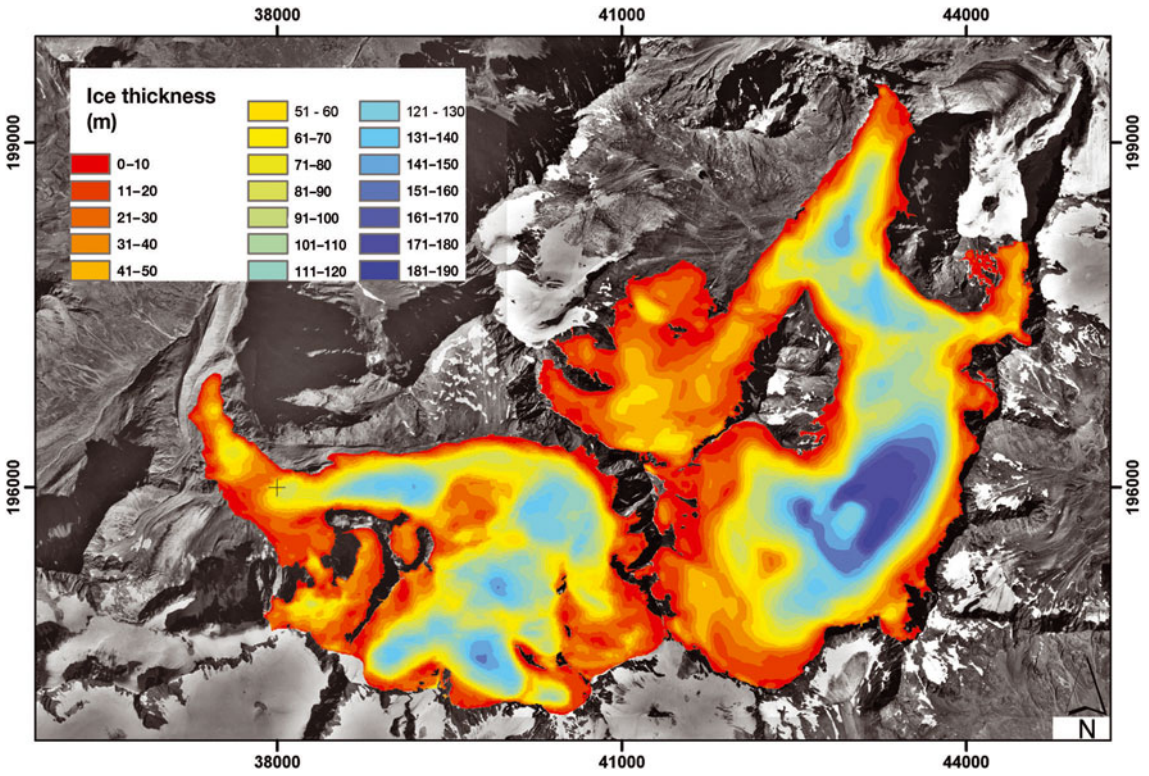

Fig. 4. Map of ice thickness of Taschachferner and Mittelbergferner calculated with the topo2raster tool.

2. the accuracy of the oscilloscope reading
3. the uncertainty of the antenna separation
4. unknown point of bedrock reflection
5. interpretation of multiple reflections.

Most of the measurements were carried out in winter, when the glacier was under seasonal snow cover. In the absence of a well-defined summer melt layer, snow probing does not allow the height of snow cover to be gauged, especially in the accumulation area. Thus the seasonal snow cover adds to the glacier thickness, in an order of 2 to ~6 m. Neglecting the signal velocities in firn (~200 m μs^{-1}) and snow (~290 m μs^{-1}) in Eqn (1) leads to an underestimation of ice thickness (Fig. 5) of up to 7 m, assuming a firn cover of 30 m and a snow cover of 5 m. In the case of winter snow cover, the overestimation of glacier volume by including the snow cover and the underestimation of the volume caused by the bulk velocity assumption can cancel each other out.

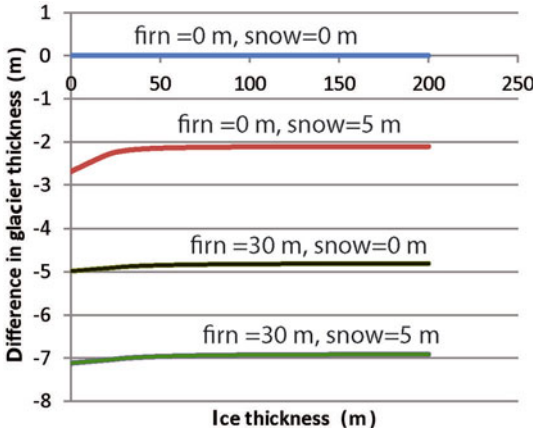

Fig. 5. Neglecting differences in signal velocities between ice, firn and snow leads to underestimation of the glacier thickness.

The accuracy of the oscilloscope reading depends on the ice thickness and is estimated at ~30 ns with the Fluke 105 B oscillosope. The effects of uncertainties 3–5 on the accuracy can be high locally, especially on steep slopes, small and deep glacier tongues or in very rough bottom topography, so they are not considered further here. Overall, the uncertainty of point ice thickness measurements is assumed to be 5%, as the spatial interpolation method is regarded as the main uncertainty.

Uncertainty of data interpolation

The ice thickness was interpolated manually, after different interpolation methods had been tested in a case study for Schaufelferner. Schaufelferner has been surveyed several times with high data density, and the volume derived by manual contouring from the sparse GPR data was similar to the high-resolution volume. Automatic spatial interpolation algorithms (e.g. kriging, spline, natural neighbour or IDW) produce zero or negative ice thickness in areas where no measurements are available. Figure 6 shows examples for Mittelbergferner and Taschachferner. Geostatistical interpolation results in significantly underestimated volumes and mean ice thicknesses (Table 1). Even when the interpolation parameters can be optimized in the example, the ice thickness remains high close to GPR point measurements and decreases in unmeasured areas to zero. Averaging the GPR-measured ice thickness biases the volume towards higher values, since flat and central parts of the glacier show higher data density than crevassed and steep areas (Table 1). For both glaciers, the average of the mean ice thickness is 45 m and the results of all spatial interpolation algorithms

https://doi.org/10.3189/2013AoG64A108 Published online by Cambridge University Press

Table 1. Results of different methods to derive the mean (h_{mean}) and maximum (h_{max}) ice thickness, with standard deviation of the ice thickness

	Taschachferner (94 GPR point meas.)			Mittelbergferner (182 GPR point meas.)		
	h_{mean}	h_{max}	std dev.	h_{mean}	h_{max}	std dev.
	m	M	m	m	m	m
Topo2raster	58	153	40	61	188	48
Kriging	24	134	38	35	170	43
IDW	23	161	39	30	151	42
Spline	36	2000	117	34	218	47
Natural neighbours	31	161	39	38	150	39
Mean GPR thickness	95	162	36	75	152	42

are within 50% of the mean. This value can be considered the upper limit of uncertainty in mean ice thickness resulting from different data interpolation algorithms.

The same interpolation algorithm was used for all glaciers. The mean uncertainty of measured ice thickness was estimated to be 5% (Fischer, 2009). Nevertheless, the main source of uncertainty in mean ice thickness is the unmeasured areas, since the mean ice thickness is calculated as the mean of all gridcells. Some gridcells are located close to measured values or known ice thickness (e.g. at the margins, where the ice thickness is zero), and should return lower uncertainties than those not surveyed. Assuming that one measured point represents a $250 \times 250\,m^2$ area with 5% uncertainty, an area-weighted mean uncertainty was calculated for the total glacier area assuming that the uncertainty in unmeasured areas is 50%.

Uncertainty of resulting volume

The uncertainty, σ_V, of the volume, V, is determined by the uncertainties, σ_h, of the mean ice thickness, h, and the uncertainties, σ_A, of the area, A.

The area change between the date of the GPR measurement and the date of the glacier inventory was corrected assuming mean ice thickness for the lost area.

For glaciers not included in GI III so far, a mean decadal area change of 15% and a mean annual surface elevation change of $-0.3\,m\,a^{-1}$ were assumed for the years between the first glacier inventory (GI I) and GI II, and $-0.9\,m\,a^{-1}$ thereafter. Thus, the overall uncertainty of the glacier volume is

$$\frac{\sigma_V}{V} = \sqrt{\left(\frac{\sigma_h}{h}\right)^2 + \left(\frac{\sigma_A}{A}\right)^2}. \quad (2)$$

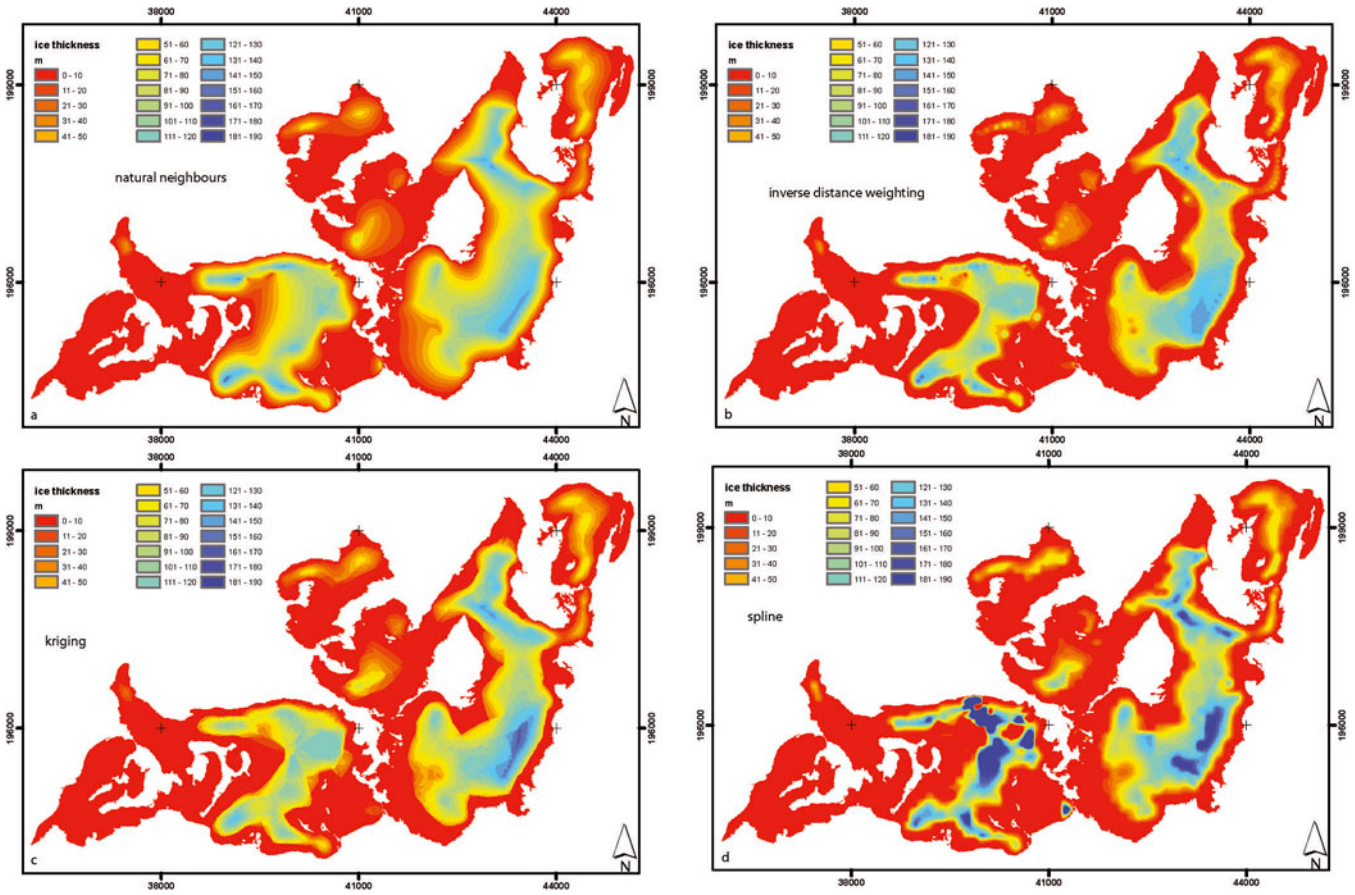

Fig. 6. Spatial interpolation algorithms as natural neighbours (a), IDW (b), kriging (c) and spline (d) underestimate ice thickness in unmeasured areas.

https://doi.org/10.3189/2013AoG64A108 Published online by Cambridge University Press

Table 2. List of surveyed glaciers with year of survey, number of point measurements (#), point measurements per square kilometre, year of glacier inventories and GPR measurements, and area (ΔA) and mean altitude (Δh) change between radar survey and DEM acquisition. For glaciers not included in GI III so far, mean values were calculated

Glacier name	#	Points km^{-2}	Year			ΔA	Δh
			GPR	GI II	GI III	km^2	m
Alpeiner Ferner	44	13	2000	1997	2006	–0.065	–2.1
Bachfallenferner	29	14	2000	1997	2006	–0.036	–2.4
Bockkogelkees O	3	5	2008	1997	2006	–0.064	–2.3
Bockkogelkees W	2	4	2008	1997	2006	–0.047	–4.0
Brandner Gletscher	12	7	2005	2002		0.045	–2.7
Brunnenkogelferner	15	10	2000	1997	2006	–0.039	–3.2
Daunkogelferner	48	35	1995	1997	2006	0.021	1.2
Fernauferner	98	58	1999	1997	2006	–0.039	–1.3
Gaisbergferner	33	28	1999	1997	2006	–0.035	–1.3
Gaißkarferner	28	55	1995	1997	2006	0.028	2.0
Gefrorene Wand Kees	89	23	1998	1999	2006	0.047	0.8
Gepatschferner	371	22	2001	1997	2006	–0.239	–2.4
Grießkogel	1	2	2008	1997	2006	–0.020	–5.6
Grinner Ferner	22	320	1996	1996		0.000	0.0
Großes Riepenkees	34	34	1998	1999	2006	0.021	0.8
Gurglerferner	100	11	1998	1997	2006	–0.096	–1.2
Hallstätter Gletscher	104	34	2009	2002		–0.331	–6.3
Hintereisferner	145	17	2001	1997	2006	–0.299	–5.4
Hochalmkees	130	45	2001	1998		–0.131	–2.7
Hochjochferner	105	15	1997	1997	2006	0.000	0.0
Hornkees	85	32	1999	1999	2006	0.000	0.0
Jamtalferner	61	16	2005	2002	2006	–0.043	–5.8
Karlesferner	23	16	2001	1997	2006	–0.042	–3.4
Kesselwandferner	213	53	1995	1997	2006	0.051	0.9
Langtaler Ferner	69	24	2005	1997	2006	–0.245	–9.6
Lüsener Ferner	36	12	2000	1997	2006	–0.038	–2.0
Lüsener Ferner Berglas	4	10	2000	1997	2006	–0.003	–1.3
Marzellferner	40	8	2002	1997	2006	–0.243	–5.9
Mittelbergferner	123	12	1998	1997	2006	–0.042	–1.1
Mullwitzkees	34	11	2003	1998		–0.243	–4.5
Niederjochferner	38	17	2002	1997		–0.165	–4.5
Nillkees	25	157	2006	1998		–0.019	–7.2
Obersulzbachkees	129	12	2001	1998		–0.495	2.7
Ochsentaler Gletscher	38	15	2000	2002	2004	0.021	5.0
Ödenwinkelkees	99	48	1998	1998		0.000	0.0
Östlicher Wannetferner	11	19	2010	1997	2006	0.052	–9.5
Pasterze	178	10	1998	1998		0.000	0.0
Rainerkees	66	19	2003	1998		–0.263	–4.5
Rettenbachferner	81	50	2007	1997	2006	–0.135	–8.9
Rotmoosferner	43	15	2006	1997	2006	–0.357	–3.8
Schalfferner	85	11	2002	1997	2006	–0.413	–6.2
Schaufelferner	115	81	1997	1997	2006	0.000	0.0
Schladminger Gletscher	68	86	2007	2002		–0.059	–4.5
Schlatenkees	58	6	2001	1998		–0.419	–2.7
Schmiedingerkees	56	41	2003	1998		–0.102	4.5
Schwarzenberg	3	2	2008	1997	2006	–0.229	–7.4
Schwarzensteinkees	67	16	1999	1999	2006	0.000	0.0
Schwarzmilzferner	25	286	2003	2000	2006	–0.011	0.0
Sexegerten	15	7	2010	1997	2006	–0.280	–8.8
Sonnblickkees	82	56	1998	1998		0.000	0.0
Sulzenauferner	30	7	2003	1997	2006	–0.049	–3.8
Sulztalferner	52	13	2001	1997	2006	–0.141	–2.3
Taschachferner W	80	13	2003	1997	2006	–0.435	–4.1
Tiefenbachferner	74	67	2007	1997	2006	–0.121	–7.6
Tisenjochferner	29	121	1997	1997		0.000	0.0
Umbalkees	116	25	2003	1998		–0.355	–4.5
Untersulzbachkees	36	10	2001	1998		–0.002	–2.7
Vermuntgletscher	34	18	2000	2002	2004	0.052	4.1
Vernagtferner	56	6	2002	1997	2006	–0.320	–5.2
Viltragenkees	32	15	2010	1998		–0.383	–10.8
Vorderer Ölgrubenferner	8	17	2010	1997		0.000	–11.7
Waxeggkees	30	9	2001	1999	2006	–0.107	–1.6
Weißseeferner	22	8	1996	1997	2006	0.012	0.7
Windacher Ferner	25	64	2005	1997	2006	–0.078	–4.2

https://doi.org/10.3189/2013AoG64A108 Published online by Cambridge University Press

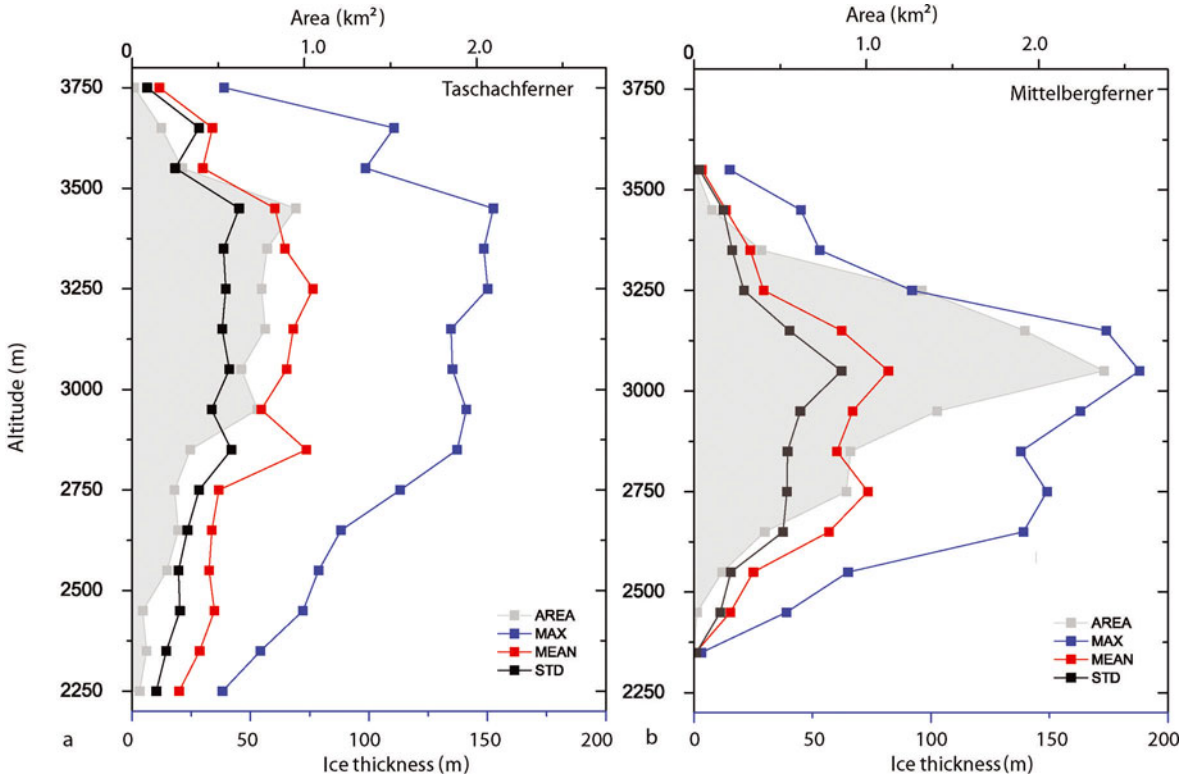

Fig. 7. Mean and maximum ice thickness and glacier area in different altitude zones of Taschachferner and Mittelbergferner.

Abermann and others (2009) estimate σ_A/A as ±1.5% for glaciers larger than 1 km^2, and ±5.0% for smaller glaciers. With the uncertainty of the mean ice thickness given above, the volume uncertainty is calculated in Table 2.

RESULTS AND DISCUSSION

For all 64 glaciers surveyed between 1995 and 2010 (Table 1) the measured data were interpolated to the total glacier area as described above. The number and spatial distribution of the measurements differ between glaciers as a result of accessibility. In crevassed areas, risky glacier travel and multiple reflections prohibited the survey. On and close to steep slopes, avalanches were a major concern, as well as fixing the antennas to the glacier surface. Figures 2 and 3 show the data recorded on Taschachferner and Mittelbergferner as typical examples of the data distribution. On Mittelbergferner, profiles along and across the glacier were measured. On Taschachferner, large crevasse zones and steep slopes prevented measurement along a central flowline. Manual interpolation of the contours of bedrock topography allowed the estimated ice thicknesses at the vertical ice walls to be included and suggests that the crevasse zones are the result of a bedrock ridge (Fig. 2).

The surveyed glaciers cover areas of 0.001–18.4 km^2. The mean thickness ranges from 10 to 92 m, and the maximum ice thickness from 26 to 311 m. For each surveyed glacier, area, mean and maximum ice thickness and the total volume are listed in Table 3. In total, the 64 glaciers cover an area of 223.3 ± 3.6 km^2 and contain a volume of 11.2 ± 1.1 km^3. This would correspond to an average ice thickness of 50 ± 3 m if the ice were equally distributed.

Not only the total volume, but also the ice thickness distribution was calculated for all glaciers. The ice thickness maps of Mittelbergferner and Taschachferner are shown in Figure 4. Ice divides and glacier areas were assumed to be the same as in the glacier inventory to allow comparisons on a glacier-to-glacier basis. The ice divides in this study are therefore not considered to be flow divides but the glacier surface water divides mapped in the 1969 glacier inventory.

All spatial data were calculated in a very dense grid, although similar studies have used a spatial resolution of 25 m (Farinotti and others, 2009a). In this study, a nominal resolution of 5×5 m was chosen to avoid artefacts caused by different grid sizes used for the surface and bedrock DEM. The spatial resolution of the data differs from glacier to glacier, dependent on the number and distribution of ice thickness measurements. A grid size between 100×100 m^2 and 250×250 m^2 would thus have been more appropriate, but would then have resulted in mismatches with the glacier inventory data, especially for smaller glaciers. For most glaciers, the ice thickness data do not allow calculation of potential subsurface glacier lakes or routing of subglacial water flows. For specific analysis of features of the subglacial topography, higher data density and, to retrieve a higher spatial resolution of the subglacial topography, higher frequencies/smaller antenna footprints are recommended. Products of the compiled GPR data useful for glaciological application are, for example, altitudinal distributions of the ice volume, as shown for Mittelbergferner and Taschachferner in Figure 7.

The number and distribution of survey points was governed by the topography of the glaciers, but since the thickest parts of the glaciers are usually located in flat areas with few crevasses, the maximum ice thickness will have been recorded for each glacier. Steep and crevassed areas usually show thinner ice cover. In some locations, the spatial coverage could be improved by helicopter surveys. In areas subject to multiple reflections (e.g. crevassed areas

https://doi.org/10.3189/2013AoG64A108 Published online by Cambridge University Press

Table 3. Areas, *A* (GI II), mean ice thickness, *h* (GI II), and volumes, *V* (GI II), calculated from the GPR data and corrected for area and volume change between the GPR measurements and the glacier inventory. The maximum ice thickness was not corrected with the local thickness change since that is not available for every glacier. The uncertainty of the maximum ice thickness, h_{max} (GPR), is therefore higher, to correspond to the GI II volume data

Glacier name	*A* (GI II)	*h* (GI II)	*V* (GI II)		h_{max} (GPR)
	km^2	m	km^3	%	m
Alpeiner Ferner	3.406 ± 0.051	51 ± 10	0.174 ± 0.035	21	163 ± 12
Bachfallenferner	2.084 ± 0.031	41 ± 7	0.086 ± 0.015	19	97 ± 10
Bockkogelkees O	0.635 ± 0.032	42 ± 16	0.027 ± 0.010	40	87 ± 18
Bockkogelkees W	0.522 ± 0.026	73 ± 29	0.038 ± 0.015	42	69 ± 33
Brandner Gletscher	1.651 ± 0.025	19 ± 5	0.031 ± 0.009	34	74 ± 8
Brunnenkogelferner	1.524 ± 0.023	27 ± 7	0.041 ± 0.010	28	56 ± 10
Daunkogelferner	1.376 ± 0.021	42 ± 4	0.057 ± 0.005	9	107 ± 5
Fernauferner	1.693 ± 0.025	37 ± 5	0.063 ± 0.009	15	178 ± 6
Gaisbergferner	1.191 ± 0.018	34 ± 2	0.041 ± 0.003	7	99 ± 4
Gaißkarferner	0.514 ± 0.026	39 ± 6	0.020 ± 0.003	15	108 ± 8
Gefrorene Wand Kees	3.818 ± 0.057	34 ± 2	0.130 ± 0.008	6	124 ± 3
Gepatschferner	17.16 ± 0.257	94 ± 5	1.618 ± 0.089	6	221 ± 7
Grießkogel	0.429 ± 0.021	20 ± 6	0.008 ± 0.003	45	55 ± 12
Grinner Ferner	0.069 ± 0.003	11 ± 8	0.001 ± 0.001	80	32 ± 8
Großes Riepenkees	0.989 ± 0.049	25 ± 2	0.025 ± 0.003	10	76 ± 3
Gurglerferner	9.379 ± 1.141	59 ± 15	0.555 ± 0.142	26	201 ± 16
Hallstätter Gletscher	3.041 ± 0.046	55 ± 4	0.164 ± 0.013	9	131 ± 10
Hintereisferner	8.55 ± 0.128	67 ± 7	0.573 ± 0.063	12	242 ± 13
Hochalmkees	2.907 ± 0.044	53 ± 6	0.152 ± 0.016	11	155 ± 8
Hochjochferner	6.829 ± 0.102	36 ± 6	0.246 ± 0.038	15	100 ± 6
Hornkees	2.665 ± 0.040	28 ± 2	0.075 ± 0.006	8	111 ± 2
Jamtalferner	3.712 ± 0.056	52 ± 6	0.192 ± 0.022	13	119 ± 12
Karlesferner	1.457 ± 0.022	26 ± 3	0.038 ± 0.005	15	70 ± 7
Kesselwandferner	4.052 ± 0.061	79 ± 11	0.320 ± 0.043	13	155 ± 11
Langtaler Ferner	2.894 ± 0.043	56 ± 3	0.156 ± 0.008	6	147 ± 12
Lüsener Ferner	3.105 ± 0.047	58 ± 13	0.180 ± 0.042	24	131 ± 15
Lüsener Ferner Berglas	0.395 ± 0.020	79 ± 21	0.031 ± 0.009	28	131 ± 23
Marzellferner	4.885 ± 0.073	52 ± 15	0.251 ± 0.071	32	187 ± 20
Mittelbergferner	9.916 ± 0.149	53 ± 11	0.526 ± 0.114	22	188 ± 13
Mullwitzkees	3.229 ± 0.048	39 ± 9	0.122 ± 0.029	26	78 ± 13
Niederjochferner	2.204 ± 0.033	31 ± 3	0.066 ± 0.006	11	98 ± 7
Nillkees	0.159 ± 0.008	22 ± 6	0.003 ± 0.001	40	42 ± 13
Obersulzbachkees	11.01 ± 0.165	40 ± 10	0.446 ± 0.112	24	208 ± 13
Ochsentaler Gletscher	2.523 ± 0.038	44 ± 8	0.111 ± 0.020	16	163 ± 13
Ödenwinkelkees	2.062 ± 0.031	50 ± 6	0.103 ± 0.012	12	167 ± 6
Östlicher Wannetferner	0.571 ± 0.029	28 ± 1	0.017 ± 0.001	8	85 ± 13
Pasterze	18.38 ± 0.276	82 ± 23	1.507 ± 0.426	28	311 ± 6
Rainerkees	3.511 ± 0.053	43 ± 3	0.148 ± 0.009	8	78 ± 11
Rettenbachferner	1.604 ± 0.024	30 ± 3	0.045 ± 0.005	13	62 ± 8
Rotmoosferner	2.878 ± 0.043	32 ± 5	0.089 ± 0.013	16	104 ± 8
Schalfferner	7.656 ± 0.115	50 ± 11	0.379 ± 0.084	25	117 ± 17
Schaufelferner	1.419 ± 0.021	26 ± 5	0.037 ± 0.007	20	94 ± 5
Schladminger Gletscher	0.794 ± 0.040	45 ± 9	0.035 ± 0.007	22	131 ± 13
Schlatenkees	9.321 ± 0.140	58 ± 20	0.536 ± 0.185	36	197 ± 22
Schmiedingerkees	1.367 ± 0.021	19 ± 2	0.026 ± 0.003	10	70 ± 7
Schwarzenberg	1.552 ± 0.023	40 ± 15	0.059 ± 0.023	46	107 ± 22
Schwarzensteinkees	4.126 ± 0.062	32 ± 4	0.132 ± 0.018	14	94 ± 4
Schwarzmilzferner	0.087 ± 0.004	12 ± 9	0.001 ± 0.001	72	35 ± 9
Sexegerten	2.157 ± 0.032	35 ± 9	0.070 ± 0.019	34	93 ± 18
Sonnblickkees	1.474 ± 0.022	35 ± 5	0.052 ± 0.007	14	142 ± 5
Sulzenauferner	4.501 ± 0.068	49 ± 16	0.219 ± 0.071	35	151 ± 20
Sulztalferner	3.986 ± 0.060	42 ± 8	0.168 ± 0.033	21	131 ± 11
Taschachferner W	6.366 ± 0.095	62 ± 13	0.392 ± 0.040	22	153 ± 17
Tiefenbachferner	1.109 ± 0.017	42 ± 6	0.044 ± 0.006	17	82 ± 13
Tisenjochferner	0.24 ± 0.012	10 ± 3	0.002 ± 0.001	31	26 ± 3
Umbalkees	4.729 ± 0.071	46 ± 3	0.212 ± 0.012	6	110 ± 7
Untersulzbachkees	3.723 ± 0.056	94 ± 26	0.349 ± 0.096	28	219 ± 28
Vermuntgletscher	1.843 ± 0.028	20 ± 2	0.036 ± 0.004	9	62 ± 6
Vernagtferner	8.839 ± 0.133	42 ± 13	0.370 ± 0.117	36	134 ± 18
Viltragenkees	2.128 ± 0.032	39 ± 5	0.074 ± 0.010	16	129 ± 15
Vord. Ölgrubenferner	0.48 ± 0.024	28 ± 2	0.013 ± 0.001	13	67 ± 14
Waxeggkees	3.346 ± 0.050	30 ± 8	0.099 ± 0.028	30	83 ± 10
Weißseeferner	2.697 ± 0.040	31 ± 10	0.084 ± 0.027	32	80 ± 11
Windacher Ferner	0.389 ± 0.019	27 ± 4	0.010 ± 0.002	17	74 ± 8

https://doi.org/10.3189/2013AoG64A108 Published online by Cambridge University Press

or areas close to bedrock), airborne radar cannot be expected to perform automatically better than ground-based measurements.

The comparison of the altitudinal distribution of ice thickness in Figure 7 demonstrates that the altitude zones with the highest mean and maximum ice thickness may differ from the zones with the largest areas. Therefore, including at least the vertical distribution of ice thickness should improve the reliability of future glacier area and volume change scenarios.

CONCLUSIONS AND OUTLOOK

Nearly two decades of GPR surveys have allowed the calculation of ice thickness data for a regional glacier sample. The data will be further extrapolated to compile a regional volume inventory. The resulting volume of $11.2 \pm 1.1\,km^3$ and the mean ice thickness of 50 m will then be extrapolated to the total Austrian glacier area, which is about twice that of the surveyed area. The surveys included a large portion of the largest glaciers, but also smaller glaciers, to be representative of Austria's glaciers. The glaciers not measured to date are either small, difficult to access, steep or crevassed. Further investigations will focus on the best method for extrapolating these data. Algorithms as presented by Farinotti and others (2009a) and Huss and Farinotti (in press) are valuable approaches to modeling regional gridded ice thickness data. The data presented in this study can also be used as validation data for these algorithms. For example, the ice thickness data could help to investigate the effect of different glacier inventory dates, which is of special concern in current glacier retreat. The strength of the presented data lies in the fact that glacier areas, surface elevations and ice thickness data are derived consistently on the basis of the same dataset and recorded within a few years.

ACKNOWLEDGEMENTS

N. Span, M. Butschek, J. Lang, M. Massimo and S. Erhart carried out part of the GPR measurements. This work would not have been possible without the many helpers during several years of campaigns. K. Helfricht and M. Stocker helped with data processing. The field campaigns on Austrian glaciers were funded by the Commission of Geophysical Research, Austrian Academy of Sciences.

REFERENCES

Abermann J, Lambrecht A, Fischer A and Kuhn M (2009) Quantifying changes and trends in the glacier area and volume in the Austrian Ötztal Alps (1969–1997–2006). *Cryosphere*, **3**(2), 205–215 (doi: 10.5194/tc-3-205-2009)

Abermann J, Seiser B, Meran I, Stocker-Waldhuber M, Goller M and Fischer A (2012) A new ALS glacier inventory of North Tyrol, Austria, for 2006. *Z. Gletscherkd. Glazialgeol.*, **43–44**, 109–119

Arendt AA, Echelmeyer KA, Harrison WD, Lingle CS and Valentine VB (2002) Rapid wastage of Alaska glaciers and their contribution to rising sea level. *Science*, **297**(5580), 382–386 (doi: 10.1126/science.1072497)

Bauder A (2001) Bestimmung der Massenbilanz von Gletschern mit Fernerkundungsmethoden und Fliessmodellierungen: eine Sensitivitätsstudie auf dem Unteraargletscher. *Mitt. VAW/ETH* 169

Binder D, Brückl E, Roch KH, Behm M, Schöner W and Hynek B (2009) Determination of total ice volume and ice-thickness distribution of two glaciers in the Hohe Tauern region, Eastern Alps, from GPR data. *Ann. Glaciol.*, **50**(51), 71–79 (doi: 10.3189/172756409789097522)

Casassa G, López P, Pouyard B and Escobar F (2009) Detection of changes in glacial run-off in alpine basins: examples from North America, the Alps, central Asia and the Andes. *Hydrol. Process.*, **23**(1), 31–41 (doi: 10.1002/hyp.7194)

Farinotti D, Huss M, Bauder A, Funk M and Truffer M (2009a) A method to estimate ice volume and ice-thickness distribution of alpine glaciers. *J. Glaciol.*, **55**(191), 422–430 (doi: 10.3189/002214309788816759)

Farinotti D, Huss M, Bauder A and Funk M (2009b) An estimate of the glacier ice volume in the Swiss Alps. *Global Planet. Change*, **68**(3), 225–231 (doi: 10.1016/j.gloplacha.2009.05.004)

Fischer A (2009) Calculation of glacier volume from sparse ice-thickness data, applied to Schaufelferner, Austria. *J. Glaciol.*, **55**(191), 453–460 (doi: 10.3189/002214309788816740)

Fischer A, Olefs M and Abermann J (2011) Glaciers, snow and ski tourism in Austria's changing climate. *Ann. Glaciol.*, **52**(58), 89–96 (doi: 10.3189/172756411797252338)

Fischer N, Span M, Kuhn M, Massimo M and Butschek M (2007) Radarmessungen der Eisdicke Österreichischer Gletscher. Band II: Messungen 1999 bis 2006. *Österreich. Beitr. Meteorol. Geophys.* 39

Haeberli W, Wächter HP, Schmid W and Sidler C (1982) Erste Erfahrungen mit dem US Geological Survey – Monopuls Radioecholot im Firn, Eis und Permafrost der Schweizer Alpen. *Arb. VAW/ETH* 6

Huss M and Farinotti D (in press) Distributed ice thickness and volume of 180,000 glaciers around the globe. *J. Geophys. Res.*,**117**(F4), F04010 (doi: 10.1029/2012JF002523)

Huss M, Farinotti D, Bauder A and Funk M (2008) Modelling runoff from highly glacierized alpine drainage basins in a changing climate. *Hydrol. Process.*, **22**(19), 3888–3902 (doi: 10.1002/hyp.7055)

Hutchinson MF (1989) A new procedure for gridding elevation and stream line data with automatic removal of spurious pits. *J. Hydrol.*, **106**(3–4), 211–232 (doi: 10.1016/0022-1694(89)90073-5)

Jansson P, Hock R and Schneider T (2003) The concept of glacier storage: a review. *J. Hydrol.*, **282**(1–4), 116–129 (doi: 10.1016/S0022-1694(03)00258-0)

Kaser G, Grosshauser M and Marzeion B (2010) Contribution potential of glaciers to water availability in different climate regimes. *Proc. Natl Acad. Sci. USA (PNAS)*, **107**(47), 20 223–20 227 (doi: 10.1073/pnas.1008162107)

Kuhn MH and Escher-Vetter H (2004) Die Reaktion der osterreichischen Gletscher und ihres Abflusses auf Anderungen von Temperatur und Niederschlag. *Österreich. Wasser. Abfallwirtsch.*, **56**(1–2), 1–7

Kuhn M and Fischer A (2012) Preliminary ice volumes of 64 Austrian glaciers based on ground penetrating radar measurements from 1996 to 2006. *Z. Gletscherkd. Glazialgeol.*, **43–44**, 121–177

Kuhn M, Lambrecht A, Abermann J, Patzelt G and Gross G (2009) *Die österreichischen Gletscher 1998 und 1969, Flächen- und Volumenänderungen.* (Landesverteidigungsakademie, Bundesministerium für Landesverteidigung Projektbericht 10) Österreichische Akademie der Wissenschaften, Wien

Kuhn M, Lambrecht A, Abermann J, Patzelt G and Gross G (2012) The Austrian glaciers 1998 and 1969, area and volume changes. *Z. Gletscherkd. Glazialgeol.*, **43–44**, 3–107

Lambrecht A and Kuhn M (2007) Glacier changes in the Austrian Alps during the last three decades, derived from the new Austrian glacier inventory. *Ann. Glaciol.*, **46**, 177–184 (doi: 10.3189/172756407782871341)

Lemke P and 10 others (2007) Observations: changes in snow, ice and frozen ground. In Solomon S and 7 others eds. *Climate change 2007: the physical science basis. Contribution of Working Group I to the Fourth Assessment Report of the*

https://doi.org/10.3189/2013AoG64A108 Published online by Cambridge University Press

Intergovernmental Panel on Climate Change. Cambridge University Press, Cambridge, 339–383

Müller F, Caflisch T and Müller G (1976) *Firn und Eis der Schweizer Alpen: Gletscherinventar.* (Geographisches Institut Publ. 57) ETH, Zürich

Müller F, Caflisch T and Müller G (1977) *Instructions for the compilation and assemblage of data for a world glacier inventory.* Temporal Technical Secretariat for the World Glacier Inventory, ETH, Zürich

Narod BB and Clarke GKC (1994) Miniature high-power impulse transmitter for radio-echo sounding. *J. Glaciol.*, **40**(134), 190–194

Radić V and Hock R (2011) Regionally differentiated contribution of mountain glaciers and ice caps to future sea-level rise. *Nature Geosci.*, **4**(2), 91–94 (doi: 10.1038/ngeo1052)

Raper SCB and Braithwaite RJ (2006) Low sea level rise projections from mountain glaciers and icecaps under global warming. *Nature*, **439**(7074), 311–313 (doi: 10.1038/nature04448)

Rose GC and Vickers RS (1974) Calculated and experimental response of resistively loaded V antennas to impulsive excitation. *Int. J. Electron.*, **37**(2), 261–271 (doi: 10.1080/00207217408900519)

Span N, Fischer A, Kuhn M, Massimo M and Butschek M (2005) Radarmessungen der Eisdicke Österreichischer Gletscher. Band 1 Messungen 1995 bis 1998. *Österreich. Beitr. Meteorol. Geophys.* 33

Stocker-Waldhuber M, Wiesenegger H, Abermann J, Hynek B and Fischer A (2012) A new glacier inventory of the province of Salzburg, Austria 2007/2009. *Z. Gletscherkd. Glazialgeol.*, **43–44**, 121–128

World Glacier Monitoring Service (WGMS) (1989) *World glacier inventory: status 1988*, ed. Haeberli W., Bösch H, Scherler K, Østrem G and Wallén C. IAHS (ICSI)/UNEP/UNESCO, World Glacier Monitoring Service, Zürich.

Wu T and King R (1965) The cylindrical antenna with nonreflecting resistive loading. *IEEE Trans. Antennas Propag.*, **13**(3), 369–373 (doi: 10.1109/TAP.1965.1138429)

Zemp M, Haeberli W, Hoelzle M and Paul F (2006) Alpine glaciers to disappear within decades? *Geophys. Res. Lett.*, **33**(13), L13504 (doi: 10.1029/2006GL026319)

https://doi.org/10.3189/2013AoG64A108 Published online by Cambridge University Press